

# Iterative Site-Based Modeling for Wireless Infrared Channels

Jeffrey B. Carruthers, *Member, IEEE*, and Prasanna Kannan

**Abstract**—We describe an iterative site-based method for estimating the impulse response of wireless infrared channels. The method can efficiently account for multiple reflections of any order. A simple geometrical model of indoor environments is presented which includes interior features such as partitions, people, and furniture, thus permitting accurate evaluation of shadowing effects. For a reflection order of three, the iterative method is over 90 times faster than the existing recursive technique. A computer implementation is described and used to demonstrate the efficiency and accuracy of the method.

**Index Terms**—Channel modeling, channel simulation, wireless infrared communications.

## I. INTRODUCTION

HIGH-QUALITY wireless access to information, networks, and computing resources by users of portable computing and communication devices is driving recent activity in indoor infrared communication [1]–[4]. High-quality access is achieved via links with low delay, high data rates, and reliable performance; and accurate characterization of the channel is essential to understanding the performance limits and design issues for wireless infrared links.

We develop a method that calculates impulse responses for wireless infrared channels formed by a transmitter and receiver placed inside a reflective environment with obstructions. The path loss and multipath dispersion for a particular link configuration will determine many aspects of communication system design, effecting in particular the appropriate modulation and coding techniques, required transmitter power and receiver sensitivities, the need for and design of channel equalization in the receiver, and the probability of bit error for digital-communication systems. Optical system properties such as transmitter power, transmitter beam shape, receiver filtering, and receiver area also need to be engineered based on these channel properties.

Electromagnetic waves at infrared or optical frequencies exhibit markedly different propagation behavior than those at radio or microwave frequencies. At radio and microwave frequencies, the dominant mode of interaction of a wave with a surface is that the surface acts as a dielectric boundary, with a reflected wave and a transmitted wave [5]. At infrared or optical frequencies, most building surfaces are opaque, which completely eliminates the transmitted wave and generally limits

the propagation of light to the transmitter's room. Furthermore, for most surfaces, the reflected light wave is diffusely reflected (as from a matte surface) rather than specularly reflected (as from a mirrored surface).<sup>1</sup> Diffraction is also an important feature of radio propagation, but it is not a significant effect at infrared frequencies as the dimensions of most building objects are typically many orders of magnitude larger than the wavelength.

These differences, as well as fundamental differences in the transmitting and receiving devices, have led researchers to develop channel and communication concepts for wireless infrared/optical systems and channels. In particular, characterization for wireless infrared channels has been done by a variety of methods at different levels. Basic system models were developed in [6], [7]. Measurement studies [7]–[9] have validated the basic diffuse reflection model and have shown the importance of the orientation of the transmitter and receiver as well as the importance of shadowing. Statistical models of channel characteristics [10] have attempted to make sense of the important factors illustrated in the above measurement studies.

Measurement studies and statistical models are useful but do not provide the same flexibility in understanding the interrelationships between the environment and the transmitter and receiver locations and orientations. Site-specific channel estimation [11]–[15] seeks efficient and accurate estimates of impulse response (the path loss and multipath dispersion) based on the propagation environment, transmitter, and receiver characteristics. The present work is an extension of Barry's method for calculating impulse responses in [11]. His recursive technique is limited to a small number of reflections or bounces  $k$ , since its compute time is exponential in  $k$ . As will be shown, the same impulse response can be computed iteratively in time proportional to  $k^2$ . As was done in [12], we generalize [11] by allowing for the inclusion of reflecting objects inside the space. In [13], a time-slicing approach is used rather than one based on reflections. In [14], a fast geometric approach is used for calculating impulse responses, but the approach is still limited by computational complexity at higher reflection orders. In [15], the authors present a mixed ray-tracing deterministic algorithm for estimating the impulse response. Their approach solves the high-order reflection problem, but introduces estimation error due to the random generation of rays. We present a completely deterministic solution which allows fast, accurate characterization of the channel in complex environments.

In the next section, we describe models for characterizing the properties of transmitters, receivers, and reflecting surfaces

Manuscript received June 8, 2001; revised December 14, 2001. This work was supported by the National Science Foundation under Grant ECS-9876149.

J. B. Carruthers is with the Department of Electrical and Computer Engineering, Boston University, Boston, MA 02215 USA.

P. Kannan is with Arraycomm, Inc., San Jose, CA 95131 USA.

Publisher Item Identifier S 0018-926X(02)05453-4.

<sup>1</sup>Diffuse reflection of light is the analog of scattering of radio waves.

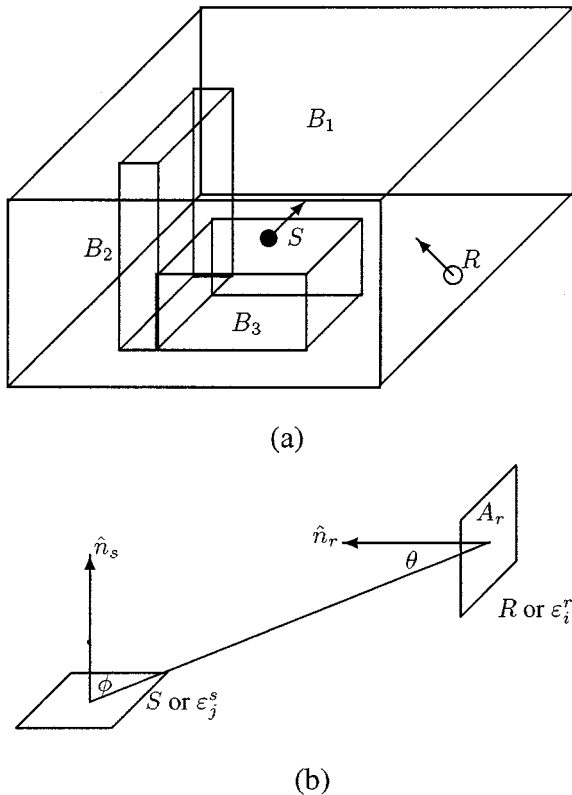


Fig. 1. Site and link model. (a) Environment. (b) Source and receiver characteristics.

within the indoor environment. In Section III, our method for impulse response calculation is outlined. The computer implementation is described in Section IV and its efficiency and accuracy are evaluated for important test cases. Conclusions are presented in Section V.

## II. SITE AND LINK MODEL

We model wireless infrared channels formed by a transmitter and receiver placed inside a reflective environment, as depicted in Fig. 1. The transmitter or source is a laser diode or a light-emitting diode transmitting a signal  $X(t)$  using intensity modulation (IM). The receiver is a photodiode with responsivity  $r$  using direct detection (DD). Hence, the received signal  $Y(t)$  is the current from the photodiode

$$Y(t) = rX(t) * h(t) + N(t) \quad (1)$$

where  $*$  denotes convolution,  $h(t)$  is the impulse response of the channel, and  $N(t)$  is noise. This baseband impulse response for IM/DD communication [7] is fixed and completely determined for a given set of source properties  $S$ , receiver properties  $R$ , and environment properties  $E$ , and hence we will write  $h(t)$  more specifically as  $h_E(t; S, R)$ .

The source  $S$  is described by a position vector  $\vec{r}_s$ , an orientation vector  $\hat{n}_s$ , and a radiation pattern  $T(\phi)$ . Throughout this paper, we restrict our attention to sources with Lambertian radiation patterns of order  $n$  given by

$$T(\phi) = \frac{n+1}{2\pi} \cos^n(\phi). \quad (2)$$

The receiver  $R$  is described by a position vector  $\vec{r}_r$ , an orientation vector  $\hat{n}_r$ , an optical collection area  $A_r$ , and an effective area at incident angles  $\theta$  of  $A(\theta) = A_r g(\theta)$ , as shown in Fig. 1(b). In this paper, we restrict our attention to receiver optical gain functions  $g(\theta) = \cos(\theta) \cdot 1\{\theta < \text{FOV}\}$  where FOV is the field of view of the receiver and  $1\{\cdot\}$  is the indicator function. The cosine dependence models decline in effective area for light incident on planar detectors at nonnormal incidence.

We model the environment  $E$  as a set of  $N_b$  rectangular boxes  $\{B_1, \dots, B_{N_b}\}$ , as shown in Fig. 1(a). The first box  $B_1$  represents the “universe” in which all other boxes and all sources and receivers are contained. This can represent a single room, a floor, or even an entire building. Interior objects are described by single boxes or combinations of boxes. This method allows for inclusion of such objects as wall partitions, doorways, desks, chairs, and people. For simplicity, we constrain the boxes so that each face is parallel to either the  $x$ ,  $y$ , or  $z$  plane. Hence, each box is described by one corner position vector  $\vec{r}_{B_i}$  and a size vector  $\{L_{x,B_i}, L_{y,B_i}, L_{z,B_i}\}$ . By definition, we place the corner of the universe at the origin and define its size vector as  $(L, W, H)$  where  $L$  is the length of the room,  $W$  is the width, and  $H$  is the height.

The boxes are further modeled as having six opaque internal faces and six opaque external faces. Only the exterior faces of the internal boxes  $B_2, \dots, B_{N_b}$  are relevant and only the internal faces of the universe box  $B_1$  are relevant, for a total of  $6N_b$  reflecting faces. Each face  $F_i$  is modeled as a diffuse reflective surface (Lambertian) of reflectivity  $\rho_{F_i}$ . For definiteness, if two faces partially overlap, the reflectivity of the shared surface is determined by the box with the larger index.

## III. IMPULSE RESPONSE CALCULATION

Our impulse response calculation follows the basic methodology outlined in [11] with extensions for an arbitrary number of boxes.

All transmitted light arriving at the receiver has undergone a definite number of reflections or bounces. Hence, we can decompose the impulse response  $h_E(t; S, R)$  as

$$h_E(t; S, R) = \sum_{k=0}^{\infty} h_E^{(k)}(t; S, R) \quad (3)$$

where  $h_E^{(k)}(t; S, R)$  is the impulse response due to signal light undergoing exactly  $k$  bounces during its path from the source to the receiver.

The line of sight (LOS) impulse response  $h_E^{(0)}(t; S, R)$  is given by

$$h_E^{(0)}(t; S, R) = V(\vec{r}_s, \vec{r}_r, E) T(\phi) (A_r g(\theta) / D^2) \delta(t - D/c) \quad (4)$$

where  $D = |\vec{r}_s - \vec{r}_r|$  is the distance between the source and the receiver. The visibility function  $V(\vec{r}_s, \vec{r}_r, E)$  is 1 when the LOS path between  $S$  and  $R$  is unobstructed, and is zero otherwise.

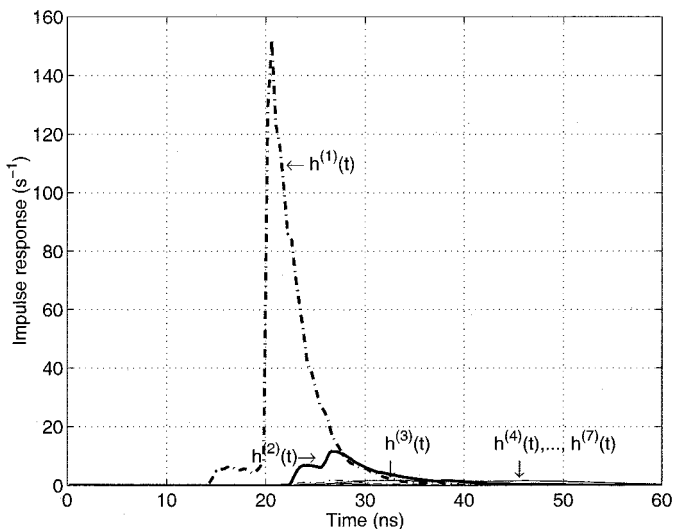


Fig. 2. Impulse responses for configuration D of [11] for various reflection orders, using the present iterative method.

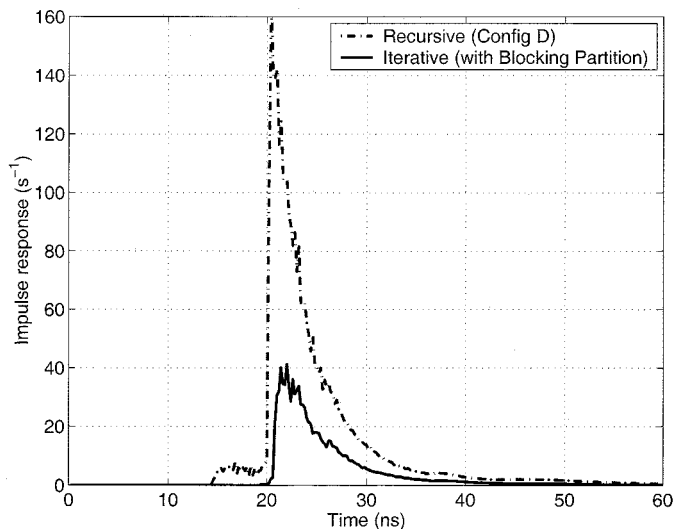


Fig. 5. The effect on impulses response of placing a partition wall between the transmitter and the receiver. The maximum reflection order is 3.

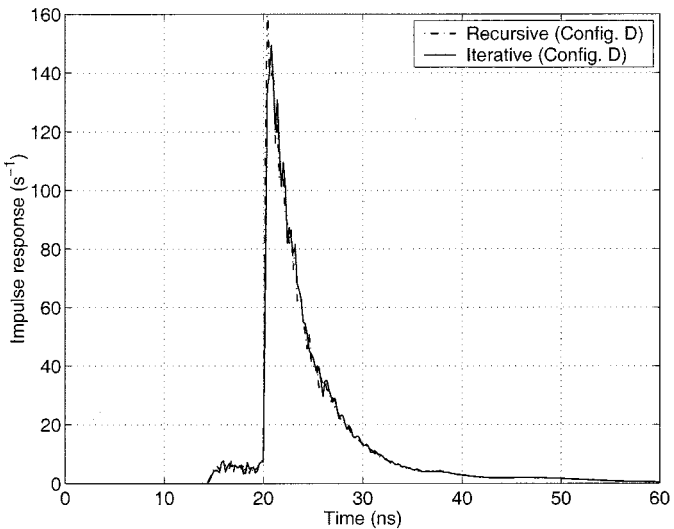


Fig. 3. Comparison of impulse responses using iterative and recursive methods for configuration D of [11]. The maximum reflection order is 3.

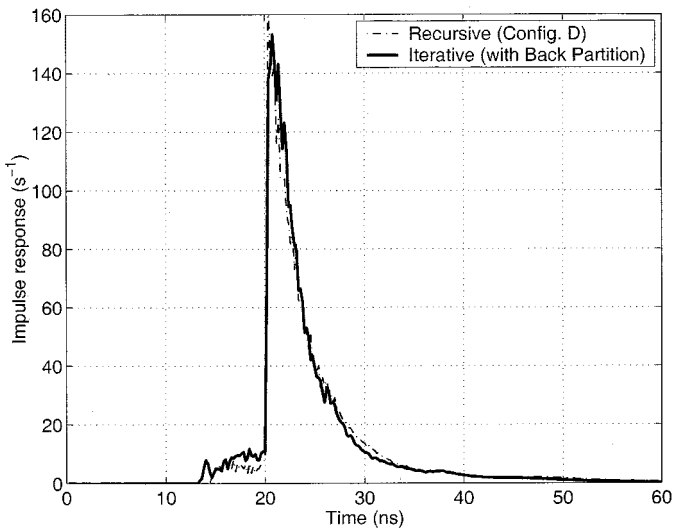


Fig. 4. The effect on impulses response of placing a partition wall behind the transmitter. The maximum reflection order is 3.

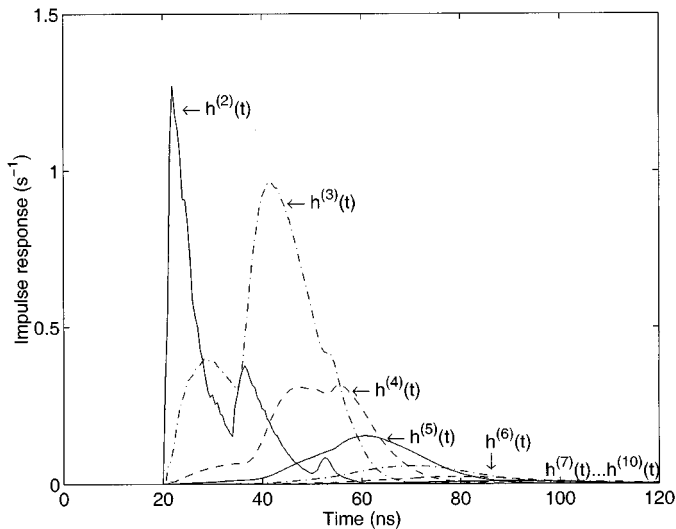


Fig. 6. Impulse responses for configuration F for various reflection orders. There is no LOS and a partition separates the source and receiver so that there is no first-bounce component.

Now, the  $k$ -bounce response can be calculated using the  $(k - 1)$ -bounce response using

$$h_E^{(k)}(t; S, R) = \int_E \rho_{d\epsilon^r} \cdot h_E^{(k-1)}(t; S, d\epsilon^r) * h_E^{(0)}(t; d\epsilon^s, R) \quad (5)$$

where the integral is over all surfaces in  $E$  and  $\rho$  is the surface reflectivity function. The quantities  $d\epsilon^s$  and  $d\epsilon^r$  represent a differential surface of area  $dr^2$  that is first acting as a receiver from the source  $S$  and then as a source to the receiver  $R$ . The surfaces act as receivers with  $g(\theta) = \cos(\theta) \cdot 1\{\theta < \pi/2\}$  and as first-order Lambertian transmitters.<sup>2</sup>

<sup>2</sup>The normal differential component  $dr^2$  does not explicitly appear in (5) since it is included implicitly in the zero-bounce calculation as the area of the source.

To estimate  $h_E(t; S, R)$  using (3), we consider only the first  $M$  bounces so that

$$h_E(t; S, R) \approx \sum_{k=0}^M h_E^{(k)}(t; S, R). \quad (6)$$

The contributions to the overall impulse response from the  $k$ -bounce impulse response will decline for increasing  $k$  so that excellent approximations can be obtained for  $M$  ranging from 3 to 10, as discussed in Section IV.

The integration in (5) is approximated by representing each face  $F_i$  at a spatial partitioning factor  $P$ , i.e., each face is divided into small elements of size  $1/P \times 1/P \text{m}^2$ . Hence, we estimate  $h_E^{(k)}(t; S, R)$  using

$$h_E^{(k)}(t; S, R) \approx \sum_{i=1}^N \rho_{\varepsilon_i^r} h_E^{(k-1)}(t; S, \varepsilon_i^r) * h_E^{(0)}(t; \varepsilon_i^s, R) \quad (7)$$

where  $\varepsilon_i^r$  and  $\varepsilon_i^s$  represent element  $i$  acting as a receiver and a source, respectively. The number of elements  $N$  is given by

$$N = 2P^2 \sum_{i=1}^{N_b} (L_{x,B_i} L_{y,B_i} + L_{y,B_i} L_{z,B_i} + L_{x,B_i} L_{z,B_i}). \quad (8)$$

Now, rather than interpreting (7) as a recursion as done in [11], we note that if we already know  $h_E^{(k-1)}(t; S, \varepsilon_i^r)$ , calculation of  $h_E^{(k)}(t; S, R)$  is a very simple operation. Indeed, since the zero-bounce impulse response is always a calculating  $h_E^{(k)}(t; S, R)$  can be accomplished by adding appropriately scaled and shifted versions of  $h_E^{(k-1)}(t; S, \varepsilon_i^r)$  together.

Hence, we apply (7) with  $R = \varepsilon_j^r$  to obtain

$$\begin{aligned} h_E^{(k)}(t; S, \varepsilon_i^r) &\approx \sum_{j=1}^N \rho_{\varepsilon_j^r} h_E^{(k-1)}(t; S, \varepsilon_j^r) * h_E^{(0)}(t; \varepsilon_i^s, \varepsilon_j^r) \\ &= \sum_{j=1}^N \alpha_{ij} h_E^{(k-1)}(t - \tau_{ij}; S, \varepsilon_j^r) \end{aligned} \quad (9)$$

where

$$\alpha_{ij} = V(\vec{r}_{\varepsilon_i^s}, \vec{r}_{\varepsilon_j^r}, E) \frac{\rho_{\varepsilon_j^r} T(\phi_{ij}) g(\theta_{ij})}{P^2 D_{ij}^2} \quad (10)$$

and  $\tau_{ij} = D_{ij}/c$ . The quantities  $\phi_{ij}$ ,  $\theta_{ij}$ , and  $D_{ij}$  are the receiver's angle to the source, the source's angle to the receiver, and the source-to-receiver delayed  $\delta$ -function distance, respectively, for the source  $\varepsilon_j^s$  and the receiver  $\varepsilon_i^r$ .

We note that evaluation of these  $N$  equations of (9) for  $k$  allows for iteration to  $k + 1$ . Hence, to calculate  $h_E^{(k)}(t; S, R)$ , we first calculate the  $N$  impulse responses  $h_E^{(1)}(t; S, \varepsilon_i^r)$ . Using these, we compute  $h_E^{(2)}(t; S, \varepsilon_i^r)$  and continue until we have  $h_E^{(k-1)}(t; S, \varepsilon_i^r)$  at which point we can directly apply (7) for the intended receiver.

#### IV. RESULTS

We have developed a computer implementation of the models and calculation methods described in Sections II and III. The

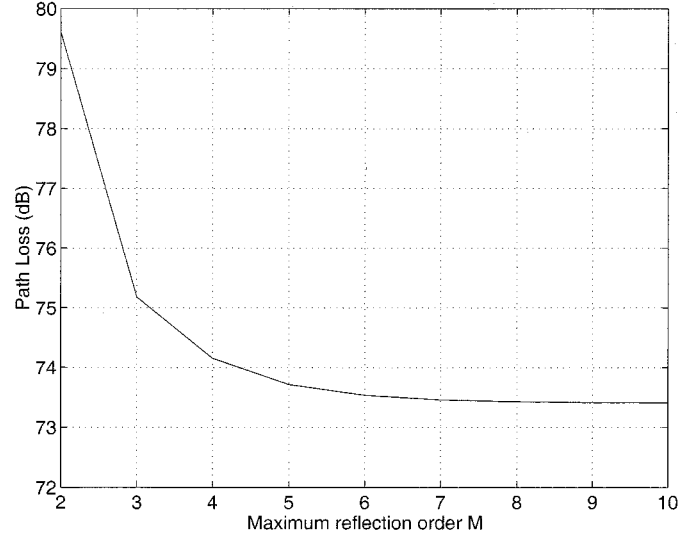


Fig. 7. Estimated path loss for configuraton F as a function of maximum reflection order.

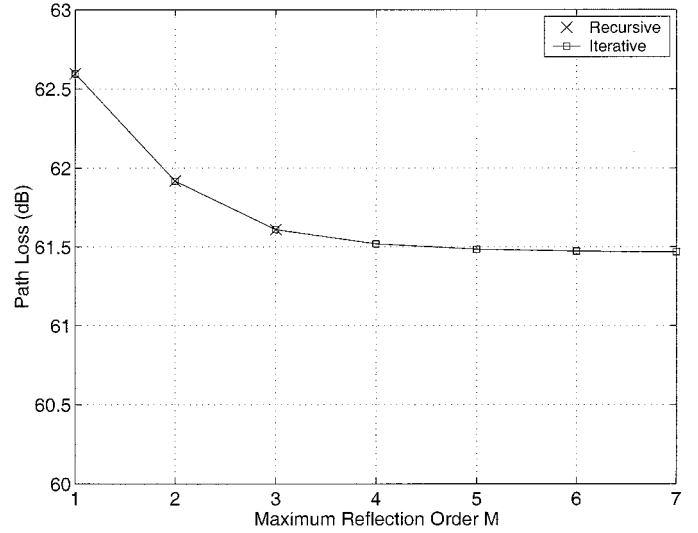


Fig. 8. Estimated path loss for configuraton D as a function of bounces. The resolution is 4.

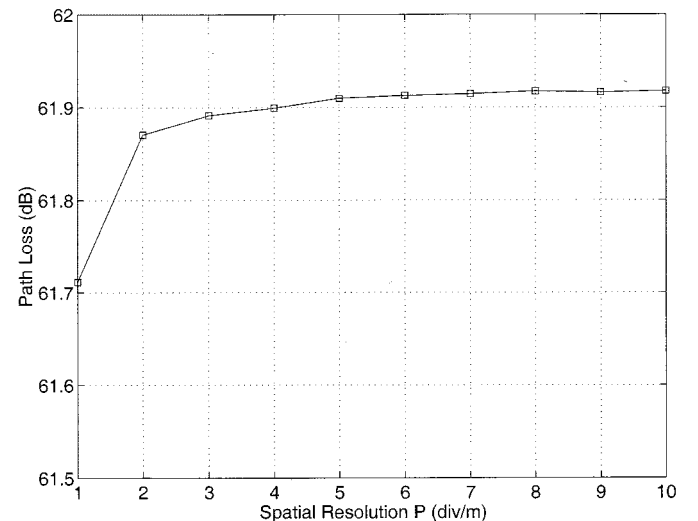


Fig. 9. Estimated path loss for configuraton D as a function of partitioning resolution for a reflection order of 2.

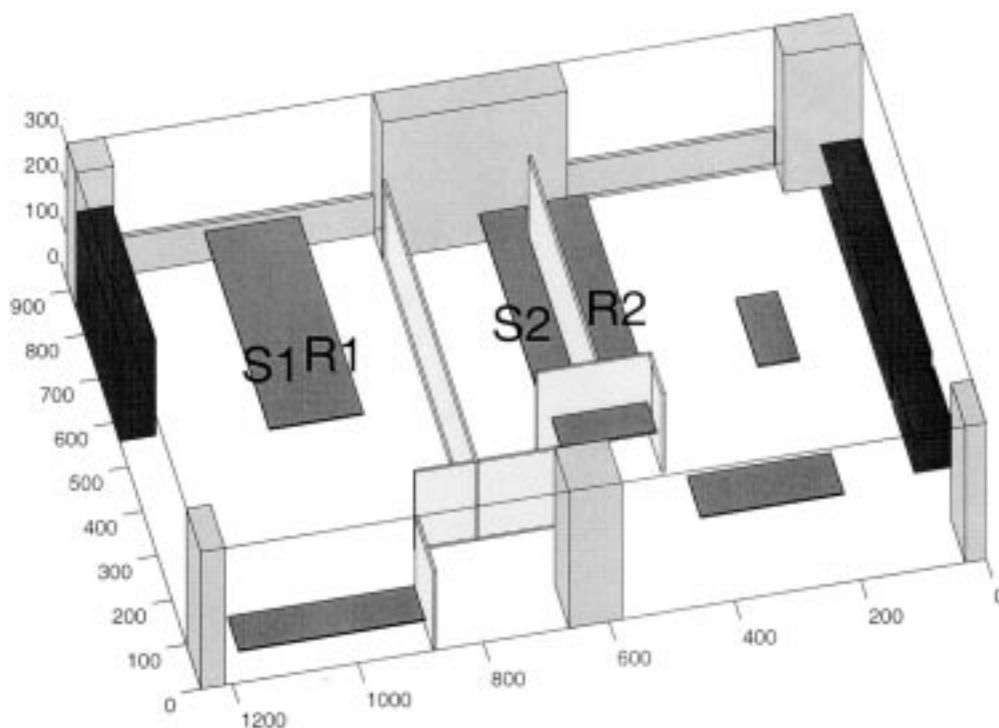


Fig. 10. Aerial view of a model of an actual research laboratory. S1 and S2 are sources, and R1 and R2 are receivers. The scale is in centimeters.

program is written in the C programming language and employs a MATLAB interface using the MEX facility and it is available from[16].

We first validate our work by considering the room entitled configuration D in [11]. The impulse responses are shown individually for the first seven reflection orders in Fig. 2. We estimate that in this configuration, the path loss is 61.6 dB if the first three bounces are considered and is 61.4 dB for the first seven bounces.

The impulse response shape and the path loss are in agreement with previously reported values, as shown in Fig. 3. This demonstrates that our method is functionally equivalent to Barry's in the simple case of empty rooms. In Figs. 4 and 5, we demonstrate the importance of being able to include room objects such as partitions. In these graphs, we compare the impulse response of an empty room with configuration D of [11] (calculated using the existing recursive method of [11]), and introduce a 2-m-high partition wall. In Fig. 4, the partition is placed behind the transmitter (relative to the receiver), which has the effect of slightly increasing the onset part of the impulse response (between 15 and 20 ns). In Fig. 5, the partition is placed between the transmitter and the receiver. This significantly increases the path loss (by 5.0-dB) and also changes the multipath shape. For example, the initial energy arriving with delay between 15 and 20 ns is eliminated, as this corresponds to a reflection from a wall near the receiver which is now blocked by the partition.

Let us examine an even more dramatic example of how furniture can influence the impulse response. We take the same room parameters  $E$  for configuration D but place the transmitter and receiver 0.5 m apart (this is configuration E).<sup>3</sup>

<sup>3</sup>The transmitter is at (3.5,1.88,1.2) and the receiver is at (4,1.88,1.2)

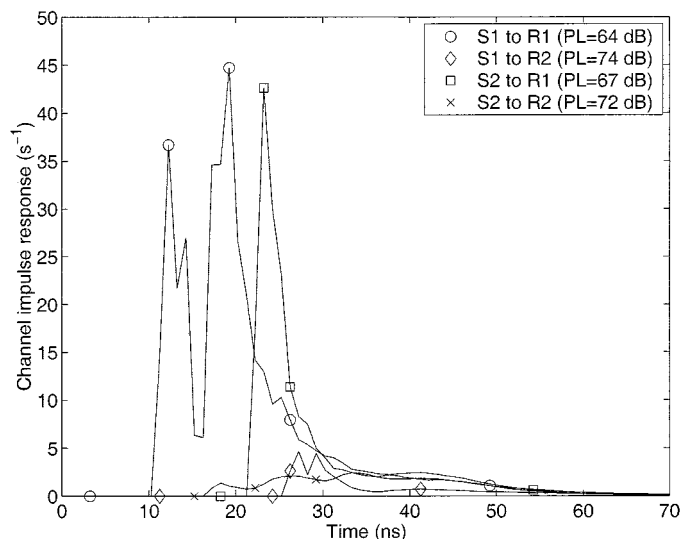


Fig. 11. Impulse responses for the room depicted in Fig. 10. Four bounces are included, and a spatial resolution of four divisions per meter (div/m) is used.

The five-bounce path loss is 58.3 dB. We now consider the addition of a 2-m-high partition between the two devices (configuration F), and plot the  $k$ -bounce impulse responses in Fig. 6 and the path loss in Fig. 7. First, we notice that the first bounce impulse response is eliminated due to shadowing from the partition, resulting in an increase of 15.2 dB in path loss. Further, for accurate path-loss estimation in this case, one needs to consider at least up to the five-bounce impulse response.

Let us consider the accuracy of the method as determined by the reflection order  $M$  used and the spatial resolution  $P$ . We consider only the path-loss estimate, as improved path-loss

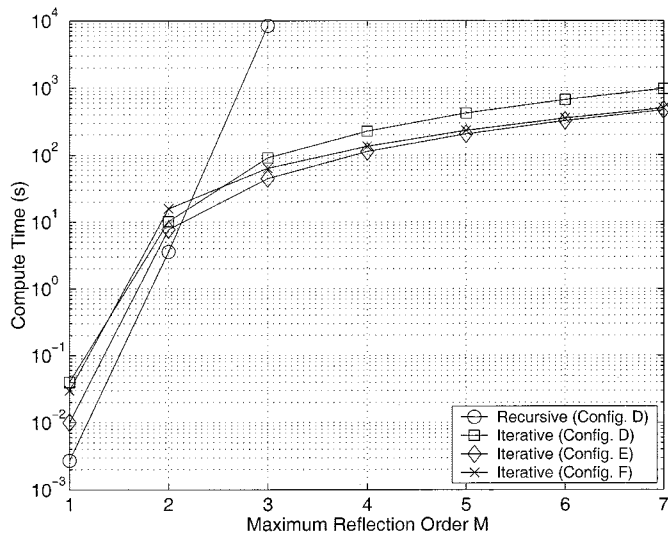


Fig. 12. Computation time for impulse responses as a function of maximum reflection order. The spatial resolution  $P$  is four divisions per meter.

estimation in this context also implies more accurate estimation of the multipath impulse response shape. In Fig. 8, we see the path-loss estimate improves as we consider more bounces and there is essentially no additional power contribution from the sixth and seventh bounce in this case. In environments with typical reflectivities and geometries, considering bounces from three to five should be sufficient for most applications. The effect of increasing the spatial resolution  $P$  for  $M = 2$  is depicted in Fig. 9. This chart shows significant improvements in accuracy as resolution is increased to four divisions per meter (div/m), and then very little improvement.

A realistic room and some characteristic impulse responses from the room are shown in Figs. 10 and 11. The room is a research lab with partitions, lab benches, desks, and closets. A total of 26 boxes are used to model the room; chairs and people are omitted. Impulse responses are calculated up to four bounces, and a spatial partitioning of four divisions per meter is used. The source receiver separations range from 1 to 5.5 m. The results show a significant impact from partitions in the room. Source S2 and receiver R2 are separated by 1.5 m and there is a path loss of 72 dB. However, S2 and receiver R1 are separated by 3 m but only suffer a path loss of 67 dB. The more distant receiver receives 5 dB more power since the partition between S2 and R1 blocks less of the ceiling than the partition between S2 and R2, even though they are the same height. Another important observation is that the path loss from S1 to R1 is 8 dB less than the path loss from S2 to R2. The difference is due to the partition between S2 and R2, which reduces the ceiling reflection.

In Figs. 12 and 13, we examine actual computation times for calculating impulse responses. These were measured on a 1-GHz Pentium III personal computer. The three-bounce impulse response for configuration D was reported to take 24 h on a 1992-vintage Sun Sparcstation 2 [11] and the recursive method on the present computer required 2.3 h. We would thus estimate that the four-bounce impulse response would require about nine months of compute time using the recursive method. Using

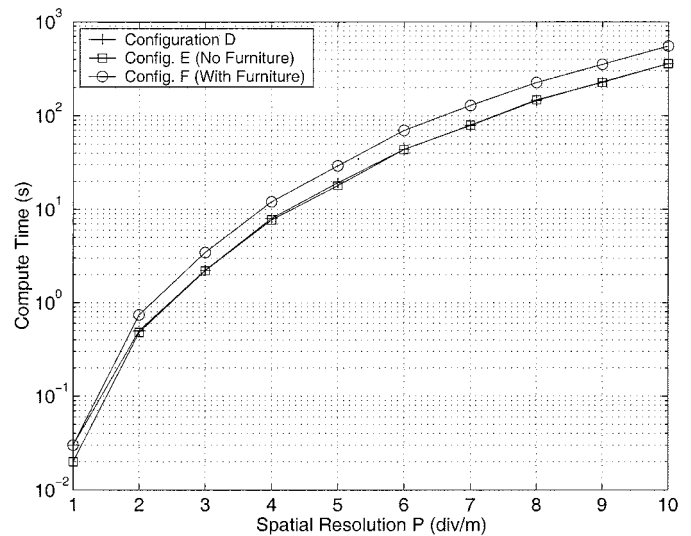


Fig. 13. Computation time for impulse responses as a function of partitioning resolution  $P$ , for maximum reflection order  $M$  of 2.

the iterative method, the three-bounce impulse response is computed in 90.7 s, or about 92 times faster. We also report results for bounces up to  $M = 7$ . The agreement between the recursive and iterative methods is illustrated in Fig. 8, where all available data points ( $k = 1, 2, 3$ ) show excellent agreement. The effect of the spatial partitioning factor on the compute time is shown in Fig. 13. Although the spatial resolution can be increased to ten div/m or more, Fig. 9 shows that spatial resolutions of more than fine divisions per meter do not significantly improve the model accuracy.

## V. CONCLUSION

Multipath impulse response estimation for wireless infrared IM/DD channels can be performed accurately and efficiently using the described iterative site-based model and computer implementation. Complex reflection environments can be modeled, which allows for inclusion of shadowing and related effects. The method can account for multiple reflections of any order and in particular makes practical the calculation of four- and five-bounce impulse responses.

## ACKNOWLEDGMENT

The authors thank Prof. J. Barry for allowing use of his original IRSIM software described in [11] as a basis for the present work, and the reviewers for their valuable suggestions.

## REFERENCES

- [1] J. M. Kahn and J. R. Barry, "Wireless infrared communications," *Proc. IEEE*, vol. 85, pp. 265–298, Feb. 1997.
- [2] D. Heatley, D. Wisely, I. Neild, and P. Cochrane, "Optical wireless: The story so far," *IEEE Commun. Mag.*, pp. 72–82, Dec. 1998.
- [3] Infrared Data Association [Online]. Available: <http://www.irda.org>
- [4] *Wireless LAN Medium Access Control (MAC) and Physical Layer (PHY) Specifications*, 1997. IEEE 802.11 Standard Working Group.
- [5] T. S. Rappaport, *Wireless Communications: Principles and Practice*. Englewood Cliffs, NJ: Prentice-Hall, 1996.
- [6] F. R. Gfeller and U. H. Bapst, "Wireless in-house data communication via diffuse infrared radiation," *Proc. IEEE*, vol. 67, pp. 1474–1486, Nov. 1979.

- [7] J. M. Kahn, W. J. Krause, and J. B. Carruthers, "Experimental characterization of nondirected indoor infrared channels," *IEEE Trans. Commun.*, vol. 43, pp. 1613–1623, Feb.–Mar.–Apr. 1995.
- [8] H. Hashemi, G. Yun, M. Kavehrad, F. Behbahani, and P. Galko, "Frequency response measurements of the wireless indoor channel at infrared optics," presented at the International Zurich Seminar on Digital Communication, Mar. 1994.
- [9] —, "Indoor propagation measurements at infrared frequencies for wireless local area networks applications," *IEEE Trans. Veh. Technol.*, vol. 43, pp. 562–576, Aug. 1994.
- [10] J. B. Carruthers and J. M. Kahn, "Modeling of nondirected wireless infrared channels," *IEEE Trans. Commun.*, vol. 45, pp. 1260–1268, Oct. 1997.
- [11] J. R. Barry, J. M. Kahn, W. J. Krause, E. A. Lee, and D. G. Messerschmitt, "Simulation of multipath impulse response for indoor wireless optical channels," *IEEE J. Select. Areas Commun.*, vol. 11, pp. 367–379, Apr. 1993.
- [12] M. Abtahi and H. Hashemi, "Simulation of indoor propagation channel at infrared frequencies in furnished office environments," in *PIMRC*, 1995, pp. 306–310.
- [13] F. Lopez-Hernandez and M. Betancor, "DUSTIN: Algorithm for calculation of impulse response on IR wireless indoor channels," *Electron. Lett.*, vol. 33, pp. 1804–1806, Oct. 1997.
- [14] D. Mavrikis and S. R. Saunders, "A novel modeling approach for wireless infrared links," in *Proc. 3rd Int. Symp. Wireless Personal Multimedia Commun. (WPSCS'00)*, 2000, pp. 609–614.
- [15] F. J. Lopez-Hernandez, R. Perez-Jimenez, and A. Santamaria, "Ray-tracing algorithms for fast calculation of the channel impulse response on diffuse IR wireless indoor channels," *Opt. Eng.*, vol. 39, pp. 2775–2780, 2000.
- [16] IrSimIt, J. B. Carruthers and P. Kannan. [Online]. Available: <http://iss.bu.edu/bwc/irsimit>



**Jeffrey B. Carruthers** (S'87–M'97) received the B.Eng. degree in computer systems engineering from Carleton University, Ottawa, ON, Canada, and the M.S. and Ph.D. degrees in electrical engineering from the University of California, Berkeley, in 1990, 1993, and 1997, respectively.

Since 1997, he has been an Assistant Professor in the Department of Electrical and Computer Engineering at Boston University, Boston, MA. From 1990 to 1991, he was with SONET Development Group of Bell-Northern Research, Ottawa. From 1992 to 1997, he was a Research Assistant at the University of California, Berkeley. His research interests include wireless infrared communications, wireless networking, and digital communications.

Dr. Carruthers received the National Science Foundation CAREER Award in 1999.



**Prasanna Kannan** received the B.E. degree in electrical engineering from Birla Institute of Technology and Science, Pilani, India, and the M.S. degree in electrical engineering from Boston University, MA, in 1999 and 2001, respectively.

From 1999 to 2001, he was a Teaching Fellow and Research Fellow in the Department of Electrical Engineering at Boston University, Boston, MA. Currently, he is a Research Engineer with Arraycomm Inc., San Jose, CA. He is involved in designing security protocols and medium access techniques for broad-band wireless systems. His research interests include information theory, cryptography, modeling and simulation of communication networks.